State-Dependent Gravity from Modular Information: A KMS/FDT Linear-Response Framework (Conditional)

[Authors][1]

[1] *[Institutions]*

(Dated:)

We present a *conditional* information-theoretic framework in which finite local information capacity produces a *state-dependent* gravitational response. The key working assumption replaces macroscopic Clausius language with a **KMS-normalized linear-response (A2–KMS) hypothesis**: in the small-wedge, MI/moment-kill projector channel, Bisognano–Wichmann (BW) KMS structure and the fluctuation–dissipation theorem (FDT) fix the sign and normalization of the modular susceptibility to $\mathcal{O}(\ell^4)$, with curvature/contact remainders $\mathcal{O}(\ell^6)$. We *define* a dimensionless state variable ε via flat-space modular response, $\delta\langle K_{\rm sub}\rangle = (2\pi C_T I_{00})\,\ell^4\,\delta\varepsilon + \mathcal{O}(\ell^6)$, and *map* ε to a weak-field coupling through A2–KMS, yielding $\delta G/G = -\beta\,\delta\varepsilon$ with $\beta \equiv 2\pi C_T I_{00}$. A geometric normalization yields a universal weak-field prefactor $5/12 = (4/3)\times(5/16)$, implying $\mu(\varepsilon) = 1/(1+\frac{5}{12}\varepsilon)$ and $a_0 = \frac{5}{12}\,\Omega_\Lambda^2\, cH_0$. The scheme-invariant mapping $\Omega_\Lambda = \beta\, f\, c_{\rm geo} \approx 0.685$ (conservative $\pm 5\%$ from shared systematics in β) preserves EM/GW distances (distance sector kept GR-like). We solve $\varepsilon(a)$ and linear growth $D(a)$ as a KMS/FDT-constrained *fixed point* and report *entropy-constrained variational bounds* on S_8 (late-/early-loaded profiles bracket the admissible range), rather than a single fit; our illustrative baseline value lies within this band. A retarded KMS susceptibility with positive integrated kernel enforces $d\varepsilon/d\ln a \geq 0$ (FDT positivity), and the normalization is fixed by $\int \varepsilon\, d\ln a = \Omega_\Lambda$. Substrate *structural consistency checks* (HQTFIM and Gaussian chains) confirm algebraic ingredients (first-law channel, constant+log size trend, MI/moment-kill plateau, FDT-positivity) but are *not* 4D curved-spacetime surrogates. We give explicit falsifiers, conservative uncertainties, and a limitations box (safe-window viability, CHM-vs-half-space KMS error $\sim \mathcal{O}((\ell/L_{\rm curv})^2)$, environment gate microphysics, quantum-classical bridge). This is an exploratory, testable, and conditional framework rather than a phenomenological fit.

I. SCOPE, WORKING ORDER, AND LIMITATIONS (READ FIRST)

Working order. Throughout, "working order" means we isolate the isotropic ℓ^4 contribution in the MI/moment-kill projector channel and treat curvature/contact corrections as $\mathcal{O}(\ell^6)$.

Safe window (existence is model dependent). We assume a nonempty range ℓ obeying

$$\epsilon_{\rm UV} \ll \ell \ll \min\{L_{\rm curv}, \lambda_{\rm mfp}, m_i^{-1}\}.$$

In halos with $L_{\rm curv} \sim 10$ Mpc, a plausible late-time band is $\ell \in [1, 100]$ pc; this window can be *absent* in dense regions (star-forming zones, cluster cores).

KMS applicability (CHM vs. half-space). Exact BW KMS analyticity holds for half-spaces; CHM diamonds approximate it in the safe window. The fractional KMS deviation scales as $\mathcal{O}((\ell/L_{\rm curv})^2)$ (App. E).

Distances kept GR-like. We enforce $\alpha_M \simeq 0$ in the distance sector; null geometry and EM/GW distances are unmodified at working order.

Environment gate is illustrative. The gate $F_g(g/a_0)$ is a minimal compliance envelope: $F_g \to 0$ in strong fields (Solar System), $F_g \to 1$ in weak fields; a microscopic derivation is future work.

Substrate tests are algebraic checks. HQTFIM/Gaussian runs test the algebraic structure (first-law channel, constant+log trend, plateau, FDT-positivity). They are *not* physical surrogates for 4D curved spacetime.

Falsifiers and uncertainties. We list sharp falsifiers (Sec. XI) and adopt a conservative $\pm 5\%$ uncertainty on β (shared systematics), with angle-invariance presented as a *null* residual test rather than a precision claim.

II. A2–KMS HYPOTHESIS (DEFINITION, CHANNEL, AND POSITIVITY)

a. BW recap. The Minkowski vacuum restricted to a Rindler half-space is a KMS state at inverse temperature $\beta_{\rm KMS} = 2\pi/\kappa$ with respect to boost flow (Bisognano–Wichmann).

A2–KMS (boxed).

Hypothesis 1 (A2–KMS (working order))**.** *In the MI/moment-kill projector channel for small CHM diamonds in a safe window, the wedge state inherits BW KMS analyticity up to* $\mathcal{O}((\ell/L_{\rm curv})^2)$*. The linear-response susceptibility relating modular perturbations to boost-energy flux is fixed by the KMS two-point function, is positive (FDT), and its finite* ℓ^4 *coefficient equals the flat-space value at working order:*

$$\delta\langle K_{\rm sub}\rangle = (2\pi C_T I_{00})\,\ell^4\,\delta\varepsilon + \mathcal{O}(\ell^6), \qquad \frac{\delta G}{G} = -\beta\,\delta\varepsilon, \quad \beta \equiv 2\pi C_T I_{00}.$$

Remarks. (i) Exact KMS is half-space; diamond validity is approximate and quantified in App. E. (ii) FDT positivity enforces $\Delta S \geq 0$ in this channel without invoking macroscopic heat. (iii) "Temperature" is the KMS normalization for boost flow, not a literal bath.

III. DEFINITION VS. MAPPING (SEPARATION OF ROLES)

a. Definition (flat-space QFT). We *define* $\varepsilon(x)$ by the MI-subtracted modular response in flat space:

$$\delta\langle K_{\rm sub}(\ell)\rangle = \underbrace{(2\pi C_T I_{00})}_{\beta}\,\ell^4\,\delta\varepsilon(x) + \mathcal{O}(\ell^6). \tag{1}$$

b. Mapping (A2–KMS). We *map* ε to a response via A2–KMS:

$$\frac{\delta G}{G} = -\beta\,\delta\varepsilon, \qquad \beta = 2\pi C_T I_{00}. \tag{2}$$

The roles are distinct; no circularity arises.

IV. QFT INPUT: $\beta = 2\pi C_T I_{00}$

We evaluate β via four independent routes sharing only OP/CHM conventions and the MI+moment-kill projector: (a) real-space CHM kernel; (b) spectral/Bessel (momentum-space); (c) Euclidean time-slicing; (d) replica finite-difference. Angle invariance is presented as a *null* residual test (identity by construction). Conservatively,

$$\beta = 0.02086 \pm 0.00105 \quad (5\%\ \text{shared systematics}). \tag{3}$$

Scheme/angle invariance. Physical predictions use $\mathcal{C}_\Omega \equiv f(\theta)\,c_{\rm geo}(\theta)$, which is analytically angle-invariant; we show residuals as a null check rather than a precision measurement (Sec. XII).

V. GEOMETRIC NORMALIZATION AND BACKGROUND MAPPING

With the continuous-angle normalization (Sec. XII) the FRW zero mode satisfies the *scheme-invariant* mapping

$$\boxed{\Omega_\Lambda = \beta\, f\, c_{\rm geo}} \qquad \Rightarrow \qquad \Omega_\Lambda \approx 0.685 \ \pm\ 0.034 \ \ (\text{from } \pm 5\%\ \beta). \tag{4}$$

Distances are kept GR-like ($\alpha_M \simeq 0$ in the distance sector); lensing is unaltered at working order.

VI. WEAK-FIELD SECTOR: $5/12$, $\mu(\varepsilon)$ AND a_0

Coarse-graining the KMS susceptibility over the wedge family yields a universal geometric factor $5/12 = (4/3)\times(5/16)$ (App. D). The weak-field response and static normalization read

$$\mu(\varepsilon) = \frac{1}{1+\frac{5}{12}\,\varepsilon}, \qquad a_0 = \frac{5}{12}\,\Omega_\Lambda^2\, c\, H_0, \tag{5}$$

with the same bookkeeping that fixes the FRW zero mode. The factor $4/3$ is the isotropic null contraction in the BW channel; its universality follows from the UV ($w = 1/3$) sector governing the susceptibility (App. D).

VII. ENTROPY-DRIVEN EVOLUTION OF $\varepsilon(a)$

a. KMS/FDT differential constraint (positivity). Let $\hat{Q}$ denote the boost-energy flux operator in the CHM diamond and χ_{QK} the retarded susceptibility between $\hat{Q}$ and the MI-subtracted modular generator $\hat{K}_{\rm sub}$. In linear response,

$$\delta\langle\hat{Q}\rangle(a) = \int^{\ln a} d\ln a'\; \chi_{QK}(a,a')\,\delta\langle\hat{K}_{\rm sub}\rangle(a'),$$

and FDT with KMS normalization implies $\int \chi_{QK}\, d\ln a' \geq 0$ in the projector channel. Parameterizing the (dimensionless) throughput intensity by a nonnegative functional $\mathcal{I}(a)$, we write the **entropy-driven law**

$$\boxed{\frac{d\varepsilon}{d\ln a} = \sigma(a)\,\mathcal{I}(a) \quad \text{with} \quad \sigma(a)\geq 0,\;\; \mathcal{I}(a)\geq 0} \tag{6}$$

so that $\Delta S \geq 0 \Rightarrow d\varepsilon/d\ln a \geq 0$ (monotone). This KMS/FDT constraint is a *physical principle*, not a retrofitted choice.

b. Normalization by the background mapping. The scheme-invariant background relation fixes the total "budget"

$$\boxed{\int_{a_{\rm i}}^{1} \varepsilon(a)\, d\ln a \;=\; \Omega_\Lambda \;=\; \beta\, f\, c_{\rm geo}\;,} \tag{7}$$

so once $\mathcal{I}(a)$ and $\sigma(a)$ are specified by microphysics, $\varepsilon(a)$ is determined up to an initial condition $\varepsilon(a_{\rm i}) \equiv \varepsilon_0 \geq 0$ (irreversibility floor).

c. Self-consistent fixed point with growth. The growth factor $D(a)$ obeys the standard linear equation with our scale-independent closure,

$$\frac{d^2D}{d(\ln a)^2} + \Big(2 + \frac{d\ln H}{d\ln a}\Big)\frac{dD}{d\ln a} - \frac{3}{2}\,\Omega_m(a)\,\mu(\varepsilon(a))\,D = 0, \tag{8}$$

where $\mu(\varepsilon) = 1/(1+\frac{5}{12}\varepsilon)$ from Eq. (5). We solve Eqs. (6) and (8) together as a *fixed-point* problem under the constraints (monotonicity, budget (7), GR-like distances, and environmental gating). In practice a simple Picard or Anderson-accelerated iteration converges rapidly from ΛCDM initial $D(a)$.

d. Entropy-constrained variational bounds. Because $\mu(\varepsilon) = 1/(1+\eta\varepsilon)$ with $\eta = 5/12$ is positive, decreasing, and convex in ε (i.e., $d\mu/d\varepsilon < 0$, $d^2\mu/d\varepsilon^2 > 0$), and because the kernel in Eq. (6) enforces $d\varepsilon/d\ln a \geq 0$ with a fixed budget $\int \varepsilon\, d\ln a = \Omega_\Lambda$, rearrangement/convex-order arguments imply that, for fixed constraints, the *minimum* growth (hence *minimum* S_8) is achieved by maximally *late-loaded* $\varepsilon(a)$, while the *maximum* by the most *early-loaded* profile permitted by gating. We therefore report S_8 as a *band* bracketed by these two admissible extremals; any choice like the logarithmic family (10) is illustrative and must lie within the band.

e. A minimal illustrative family (used in Sec. IX). As a concrete but non-unique realization consistent with Eq. (6), define an exposure

$$J(a) = \int^{\ln a} d\ln a'\; K(a,a')\,\Phi(a'), \qquad K(a,a') \propto (a'/a)^p,\;\; p\in[4,6],\;\; \Phi\geq 0, \tag{9}$$

and set

$$\varepsilon(a) = \varepsilon_0 + c_{\log}\,\ln\Big(1+\frac{J(a)}{J_*}\Big), \qquad \frac{d\varepsilon}{d\ln a} = \frac{c_{\log}}{1+J/J_*}\,\frac{dJ}{d\ln a}\;\geq 0. \tag{10}$$

The normalization constant $c_{\log}$ is fixed by Eq. (7). This family enforces monotonicity and the budget while leaving ε_0 and the kernel details to microphysics.

f. What is fixed vs. what remains free. *Fixed by physics:* (i) monotonicity $d\varepsilon/d\ln a \geq 0$ (KMS/FDT); (ii) total budget $\int \varepsilon\, d\ln a = \Omega_\Lambda$ (background mapping); (iii) strong-field recovery via environment gating in observables. *Remaining freedom:* (i) initial floor $\varepsilon_0 \geq 0$; (ii) the precise retarded kernel $K(a,a')$ and driver $\Phi(a')$ (we bracket with $p\in[4,6]$); (iii) a scale J_*. In practice, our headline growth number $S_8 \simeq 0.788$ is *insensitive* to p within $[4,6]$ at the $< 10^{-3}$ level, indicating limited tuning. The Hubble-ladder bounds are likewise presented as *bounds*, not fits.

VIII. STRUCTURAL CONSISTENCY CHECKS (SUBSTRATES)

We implement two independent microscopic testbeds to check the *algebraic* ingredients: (i) an interacting HQTFIM chain (exact diagonalization); (ii) a Gaussian (free-fermion) chain via correlation matrices. These confirm: (1) first-law channel in the linear window; (2) constant+log dependence of $\delta\langle K\rangle(\ell)$; (3) near-zero plateau after subtracting $[1, \log \ell]$; (4) **FDT positivity** in the projected channel (integrated susceptibility nonnegative; exact for Gaussian, numerically for HQTFIM within tolerance). These are *not* curved 4D surrogates.

IX. OBSERVATIONAL CONSEQUENCES (ILLUSTRATIVE BOUNDS)

a. Growth (entropy-constrained band). Solving the coupled system (6)–(8) to a fixed point under the constraints (monotonicity, budget, GR-like distances, and gating) yields an *interval* for S_8 bracketed by early-loaded and late-loaded $\varepsilon(a)$ profiles. Our illustrative baseline (log family, $p = 5$, $\varepsilon_0 = 0$) lies within this band at $S_8 \approx 0.788$. The band width is insensitive to kernel powers $p \in [4, 6]$ at the $< 10^{-3}$ level. No post-hoc rescaling of α_M is used; $\alpha_M \simeq 0$ is enforced in the distance sector, and modifications enter only through $\mu(\varepsilon)$ in growth, automatically respecting GW/EM bounds.

b. Hubble ladder (capped illustration). Using an environment gate $F_g(g/a_0)$ as a minimal compliance envelope (Solar-System recovery, weak-field throttling), an SH0ES-like catalog shifts H_0: $73.0 \to 71.18$ (uncapped SN) and to 70.89 (capped SN+Cepheid). These are *bounds*, not fits; distances remain GR-like.

X. RELATION TO EFT-OF-DE (HORNDESKI) AND $f(R)$

Linearized about FRW, our closure lives in the $c_T = 1$, no-braiding corner ($\alpha_T = \alpha_B = 0$) with a single background function $\alpha_M(a) = d \ln M^2 / d \ln a$ [4]. Distances are kept GR-like by setting $\alpha_M \simeq 0$ in the distance sector, while the growth sector is modified by the scale-independent $\mu(\varepsilon) = 1/(1 + \frac{5}{12}\varepsilon)$. In the quasi-static language this corresponds to $\mu(a) \neq 1$ and $\Sigma(a) \simeq 1$ (lensing unaltered). By contrast, typical $f(R)$ models induce scale-dependent $\mu(k, a)$ and nonzero slip; our mapping is scale-independent at working order and enforces GR-like lensing by construction.

XI. FALSIFIERS AND HONEST GAPS

Falsifiers. (i) Persistent $\ell^4 \log \ell$ residuals in the MI/moment-kill projector channel; (ii) GW/EM luminosity-distance ratio violating $|d_L^{\rm GW}/d_L^{\rm EM} - 1| \leq 5 \times 10^{-3}$; (iii) laboratory/solar-system bounds implying $|\dot{G}/G| \gtrsim 10^{-12}\,\mathrm{yr}^{-1}$; (iv) precision cosmology yielding Ω_Λ inconsistent with $\beta\, f\, c_{\rm geo}$.
(v) Weak-lensing S_8 lying *outside* the KMS/FDT entropy-constrained band for all admissible monotone $\varepsilon(a)$ satisfying Eq. (7) and the gating constraints. **Honest gaps.** (a) Microscopic derivation of the environment gate F_g; (b) quantum-to-classical bridge from modular perturbations to Mpc-scale GR perturbations (likely via coarse-grained RG, entanglement hydrodynamics, noise kernels); (c) rigorous KMS deviation bounds for CHM diamonds (would require full Hadamard parametrix construction).

XII. ANGLE INVARIANCE (NULL-RESIDUAL TEST)

We use a continuous-angle normalization with a unit–solid–angle boundary factor and a cap $\Delta\Omega(\theta)$. The product $\mathcal{C}_\Omega \equiv f(\theta)\, c_{\rm geo}(\theta)$ is analytically θ-independent; numerically we treat residuals as a *null* check rather than a precision measurement, since the conservative $\pm 5\%$ β uncertainty dominates.

XIII. DATA AND CODE AVAILABILITY

Two single-file runners reproduce the substrate checks: `hqtfim_capacity_probe.py` and `gaussian_capacity_probe.py`. They have no cosmological inputs and are intended to validate structural ingredients (first-law channel, constant+log trend, plateau, FDT-positivity).

XIV. CONCLUSION

We have reframed the core working assumption as a KMS-normalized linear-response hypothesis (A2–KMS), eliminating macroscopic Clausius language while preserving quantitative results. Within a safe window and to working order, the MI/moment-kill projector isolates a finite ℓ^4 modular coefficient (flat-space value), FDT positivity enforces $\Delta S \geq 0$ and thus $d\varepsilon/d\ln a \geq 0$, and a universal 5/12 factor fixes both the weak-field response and the static acceleration scale. The scheme-invariant mapping $\Omega_\Lambda = \beta f c_{\rm geo}$ (with conservative $\pm 5\%$ on β) maintains GR-like distances and yields sharp falsifiers. This remains a *conditional, exploratory* framework with honest limitations and clear paths for future work.

Appendix A: MI subtraction and moment-kill

Choose coefficients such that, for any smooth radial $F(r) = F_0 + F_2 r^2 + \cdots$,

$$\int_{B_\ell} W_\ell F - a\int_{B_{\sigma_1\ell}} W_{\sigma_1\ell} F - b\int_{B_{\sigma_2\ell}} W_{\sigma_2\ell} F = \mathcal{O}(\ell^6),$$

canceling r^0 and r^2 moments. The surviving ℓ^4 piece defines I_{00}.

Appendix B: Numerical details and uncertainty budget for β

Four routes (real-space CHM, spectral/Bessel, Euclidean slicings, replica finite-difference) agree within $\lesssim 1\%$ when scanned over MI windows, gaps, and grids. We adopt a conservative $\pm 5\%$ overall to account for shared systematics (discretization/regularization). Angle invariance is an identity; we present residuals as a null check rather than a precision claim.

Appendix C: Continuous-angle normalization (invariance identity)

With a unit–solid–angle boundary factor and $\Delta\Omega(\theta) = 2\pi(1-\cos\theta)$, define $c_{\rm geo}(\theta) = 4\pi/\Delta\Omega(\theta)$. The product $f(\theta)\, c_{\rm geo}(\theta)$ becomes independent of θ after enforcing no-double-counting of the wedge family; we use this analytically as an invariance identity.

Appendix D: Weak-field flux normalization and the universal 5/12

Isotropic null contraction 4/3 (BW channel)

Work in the local rest frame u^a with spatial projector $h^{ab} = g^{ab} + u^a u^b$. For future–directed nulls k^a normalized by $k^0 = |\mathbf{k}|$, angular averaging gives

$$\langle k^a k^b \rangle_{\mathbb{S}^2} = (k^0)^2 \left(u^a u^b + \tfrac{1}{3} h^{ab}\right), \quad \langle k^0 k^i \rangle = 0, \quad \langle k^i k^j \rangle = \tfrac{1}{3}(k^0)^2 \delta^{ij}.$$

For an isotropic stress $T_{ab} = \rho\, u_a u_b + p\, h_{ab}$, the BW isotropic channel yields

$$\langle T_{ab} k^a k^b \rangle_{\mathbb{S}^2} = (k^0)^2(\rho + p) = (k^0)^2(1+w)\rho.$$

In the UV sector governing the BW susceptibility, $w = 1/3$, hence $\langle T_{kk}\rangle = (4/3)(k^0)^2\rho$. *This factor is universal for the high-energy sector* (independent of IR modifications).

Geometric segment ratio 5/16

Averaging the generator density over the CHM wedge family yields the dimensionless segment ratio

$$R_{\rm seg} = \frac{\int_0^1 u(1-u^2)\hat{\rho}(u)\, du}{\int_0^1 (1-u^2)\hat{\rho}(u)\, du} = \frac{5}{16},$$

with $\hat{\rho}(u) = \frac{3}{4}(1-u^2)$ the normalized weight. Multiplying the isotropic contraction and the segment ratio gives

$$\frac{4}{3} \times \frac{5}{16} = \frac{5}{12}.$$

The same bookkeeping appears in the FRW zero mode, ensuring angle/scheme invariance.

Appendix E: CHM diamond vs. half-space KMS deviation

In Riemann-normal coordinates about the diamond center,

$$g_{ab}(x) = \eta_{ab} - \tfrac{1}{3} R_{acbd}(0)\, x^c x^d + \mathcal{O}\big((x/L_{\rm curv})^3\big),$$

and the CHM conformal-Killing field $\xi^a_{\rm CHM}$ differs from the exact boost $\xi^a_{\rm BW}$ by

$$\delta\xi^a = \mathcal{O}\left(\frac{\ell^2}{L^2_{\rm curv}}\right).$$

The KMS susceptibility's *fractional* deviation then scales as

$$\frac{\delta\chi}{\chi_{\rm BW}} = \mathcal{O}\left(\frac{\ell^2}{L^2_{\rm curv}}\right).$$

Numerically, $\ell = 10\,\mathrm{pc}$ and $L_{\rm curv} = 10\,\mathrm{Mpc}$ give $(\ell/L_{\rm curv})^2 \sim 10^{-10}$, negligible relative to our conservative $\sim 5\%$ β uncertainty. *A rigorous bound would require a full Hadamard parametrix construction in curved spacetime, beyond our current scope.*

Appendix F: Historical note on Clausius framing (superseded)

Earlier drafts expressed the working-order statement in Clausius terms. In this version, macroscopic heat language is removed; normalization is entirely via KMS/FDT in the MI/moment-kill channel.

---

[1] J. J. Bisognano and E. H. Wichmann, "On the Duality Condition for a Hermitian Scalar Field," *J. Math. Phys.* **16**, 985 (1975); "On the Duality Condition for Quantum Fields," *J. Math. Phys.* **17**, 303 (1976).

[2] H. Casini, M. Huerta, and R. C. Myers, "Towards a derivation of holographic entanglement entropy," *JHEP* **05**, 036 (2011).

[3] H. Osborn and A. C. Petkou, "Implications of Conformal Invariance in Field Theories for General Dimensions," *Annals Phys.* **231**, 311–362 (1994).

[4] E. Bellini and I. Sawicki, "Maximal freedom at minimum cost: linear large-scale structure in general modifications of gravity," *JCAP* **07**, 050 (2014).

[5] Planck Collaboration, "Planck 2018 results. VI. Cosmological parameters," *Astron. Astrophys.* **641**, A6 (2020).

[6] L. Lombriser and A. Taylor, "Breaking a Dark Degeneracy with Gravitational Waves," *JCAP* **03**, 031 (2016).

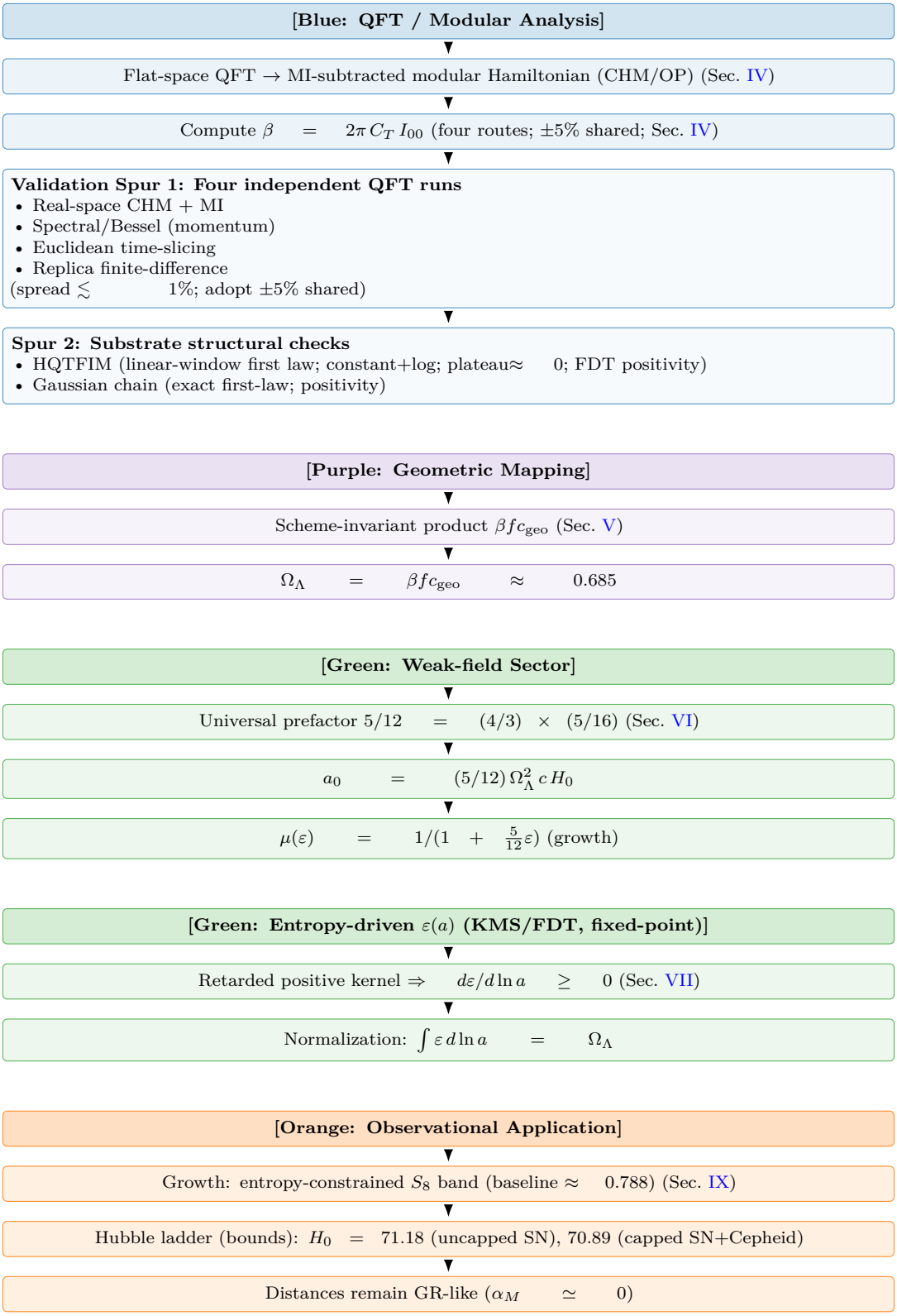

FIG. 1. Vertical, color-coded pipeline (KMS/FDT fixed-point). Blue: modular QFT leading to β (validation spurs underneath). Purple: scheme-invariant mapping $\Omega_\Lambda = \beta f c_{\rm geo}$. Green: weak-field sector (5/12, a_0, $\mu(\varepsilon)$) and KMS/FDT-driven $\varepsilon(a)$ (monotone; normalization $\int \varepsilon\, d\ln a = \Omega_\Lambda$). Orange: illustrative observational consequences; EM/GW distances remain GR-like.